Rare Metal Materials and Engineering
Volume 49, Issue 8, August 2020
Available online at www.rmme.ac.cn

Science Press

Cite this article as: Rare Metal Materials and Engineering, 2020, 49(8): 2649-2657.

ARTICLE

Microstructure and Mechanical Property of Multilayered Niobium/Zirconium Composites Processed by Accumulative Roll Bonding

Zhu Mingwei[1], Fan Zhen[2], Xu Chengjie[2], Jia Nan[2]

[1] Shenyang Aerospace University, Shenyang 110136, China; [2] Key Laboratory for Anisotropy and Texture of Materials, Ministry of Education, Northeastern University, Shenyang 110819, China

Abstract: The multilayered niobium/zirconium (Nb/Zr) composites with different initial Zr thicknesses were processed by accumulative roll bonding (ARB). Microstructure, texture and mechanical property of the composites at different ARB cycles were investigated. The results show that the heterophase interfaces are well bonded and no intermetallic compounds form. With increasing ARB cycles, shear bands form cutting through the multiple metal layers. Necking and fracture of the Zr layers occur preferentially in the composites with an initial Zr thickness of 1 mm. Dislocation cell structures are predominated in Nb layers, while a mixture consisting of grains with dense dislocations and dynamically recovered grains with a low dislocation density are predominant in Zr layers. In addition, texture evolution in Nb layers changes with varied initial thickness of Zr. When the initial Zr thickness is 1 mm, strong Cube orientation appears in Nb layers. However, when the initial Zr thickness is 2 mm, rotated-Cube is the dominant texture in Nb layers with increasing ARB cycles. The textures in Zr layers are similar in the composites with different initial Zr thicknesses. After the first ARB cycle, the $\{10\bar{1}3\}<30\bar{3}2>$ orientation is the dominant texture. With increasing ARB cycles, this orientation is slightly weakened and minor $\{11\bar{2}0\}$ fiber texture develops. With the increase of the ARB cycles, both yield strength and ultimate tensile strength increase monotonically for the composites with different initial Zr thicknesses. However, the maximum elongation firstly decreases and then increases with increasing ARB cycles. After the third ARB cycle, the maximum elongation reaches 14.2% and 16.5% for the composites with the initial Zr thicknesses of 1 and 2 mm, respectively. The high strength and good plasticity of the composites originate from the significant grain refinement in the individual metals and the recovered Zr grains during ARB, together with the featured texture evolution in the Zr layers.

Key words: accumulative roll bonding; Nb/Zr multilayered metallic composite; texture; plastic deformation

Multilayered metallic composites composed of alternatively stacked metal sheets with the certain layer thicknesses have been widely applied in many fields including micro-device, microelectro-mechanical system, biological materials and nuclear industry, owing to their high strength/hardness and good radiation damage resistance[1-3]. For the multilayered composites with the single layer thickness of the micron or even nanometer scale, the heterophase interfaces between the constituent metals may act as a tank effectively absorbing vacancies and interstitials induced by nuclear radiation[4,5]. These composites normally undergo large plastic deformation and cyclic loading under machining and the ensuing service, which sets a high demand for the resistance to deformation damage.

Considering that the low-symmetric hexagonal close-packed (hcp) metals are with the merits of low density, high strength/stiffness, and large electrical and thermal conductivity, etc.[6-9], the multilayered composites consisting of hcp metals (e.g. Zr, Ti and Mg) have attracted great interest in recent years[4,5,7-13]. However, the low ductility of hcp metals

Received date: August 28, 2019
Foundation item: National Natural Science Foundation of China (51571057, 51922026); Fundamental Research Funds for the Central Universities (N170204012); Liaoning Natural Science Foundation (20180510010)
Corresponding author: Jia Nan, Ph. D., Professor, Key Laboratory for Anisotropy and Texture of Materials, Ministry of Education, School of Material Science and Engineering, Northeastern University, Shenyang 110819, P. R. China, Tel: 0086-24-83691570, E-mail: jian@atm.neu.edu.cn

limits the application of such composites, in comparison with those consisting of high-symmetric face-centered cubic (fcc) and/or body-centered cubic (bcc) metals. Thus, the investigation on the deformation microstructures and mechanical properties for the multilayered metallic composites composed of hcp metals is very important for the design and application of the materials.

At present, multilayered metallic composites are mainly prepared by magnetron sputtering, spray deposition, explosion welding and accumulative roll bonding (ARB). By repetitive rolling and mutual stacking the metal sheets, a close welding between the constituent metals can be reached in ARB process. This method is economically viable and can effectively increase the strength of metals and alloys by grain refinement, which makes it the most potential method for the industrial processing of multilayered composites[14,15]. However, for the hcp metal sheet that has undergone rolling deformation, the strong {0001} basal texture forms and limits the number of the activated slip systems. This significantly deteriorates the uniform deformation ability of the composites fabricated by ARB. On the other hand, as it is difficult to obtain a composite consisting of dissimilar metals with a significant difference in yielding strength and work hardening ability through ARB, the processing method is majorly applied to the fabrication of fcc/fcc (e.g. Cu/Al[16]) and fcc/bcc (e.g. Cu/Nb[17,18], Cu/Ta[19] and Ni/Fe[20]) composites. Therefore, the investigations on micromechanical behavior and mechanical property of the multilayered metallic composites are mainly limited to the above-mentioned material systems and only a little research work has been conducted for the composites consisting of hcp metals[21-26]. The latter composites produced by ARB usually show a small elongation and the inversion relationship between strength and plasticity restricts the application of the composites. The investigation on AZ31 magnesium alloy fabricated by ARB at 300 °C showed that dynamically recovered recrystallization lead to the significant grain refinement after the third ARB cycle[22]. This raised the plastic elongation from 14.2% at the initial stage to 32.1% for the rolled material, whereas the strength decreases with the increasing ARB number. The study on a multilayered Al-Mg composite prepared by ARB at 400 °C showed the opposite trend after the third ARB cycle[2], i.e., the strength of the composite increased with the increasing ARB cycles. This originated from the texture evolution and dynamic recrystallization during ARB, at the expense of the decrease in elongation from 8% to 2.2% due to the formation of basal texture in the processing. Consistent phenomena have also been reported for an ME20 magnesium alloy fabricated by ARB[24].

As mentioned above, the existence of texture may have a significant effect on the micromechanical behavior of hcp metals. Thus the weakening of the basal texture is favorable for the improvement in plasticity for magnesium alloy with the introduction of shear deformation by asymmetrical rolling[27], pre-rolling the RD-ND plane[28] and the addition of RE element in the materials[29]. Then, for the multilayered composites composed of hexagonal and cubic metals, how do the constituent metals accommodate with each other and how does the stress state at the heterophase interfaces affect the mechanical property of the bulk composites? Furthermore, the interaction between the constituents will necessarily affect the texture evolution in each metal. Then it is unknown whether the texture change in the hexagonal metal is helpful for the improvement of bulk plasticity. These questions have not been answered by either experiments or theoretical calculations in previous work. However, the solutions to the questions are decisive for the successful development of hexagonal multilayered composites with a combination of high strength and good plasticity. Here, we fabricate the multilayered composites composed of bcc Nb and hcp Zr by ARB processing. The reasons of selecting this bcc/hcp composite are: First, in recent years the Zr-based composites and alloys show great advantage in nuclear industry, owing to their high strength at high temperatures and small capture cross-section for thermal neutrons[30]. Second, the previous studies on this multilayered material system mainly concentrate on structure, radiation tolerance and superconductivity, whereas the strengthening mechanism of the composite is still lacking[31,32]. In the present work, the microstructure, texture and mechanical property of the Nb/Zr composites with specific Zr thicknesses during ARB are investigated. By revealing the effect of heterophase interfaces on texture evolution of each constituent metal as well as on mechanical property of the bulk composites, the present work is favorable for the design and application of the multilayered composites composed of hcp metals.

1 Experiment

Multilayered metallic composites composed of bcc Nb and hcp Zr were fabricated with the ARB method. The raw materials were commercially pure Nb (99.8% purity) and pure Zr (99.8% purity) sheets at the annealed state, both showing equiaxed grains with the average grain size of 30~50 μm. The metal plates were firstly cut into small pieces of 120 mm×50 mm and wire brushed, followed by ultrasonic cleaning in acetone. Then 1 mm-thick Nb plate and 1 mm-thick or 2 mm-thick Zr plates were mutually stacked to obtain two sandwiched structures of Nb-1 mm/Zr-1 mm and Nb-1 mm/Zr-2 mm, with Nb plates lying at the outmost side of the stacked composites. The stacked plates were then annealed at 300 °C in a vacuum furnace (10^{-2} Pa) and rolled immediately after taking out of the furnace, reaching a nominal thickness reduction of 65% after one single rolling pass. This procedure produced the first ARB processed composite. The composite was subsequently cut into two pieces of equal area. Then the processes of surface cleaning, stacking, and single-pass roll bonding with a thickness reduction of ~65% were iterated up

to 2 and 3 cycles. An intermediate annealing treatment was performed at 575 °C for 60 min before the second and the third ARB cycles separately. Table 1 shows the total number of metal layers within the composites processed by different ARB cycles, the corresponding nominal layer thickness, and the equivalent true strain.

The sample coordinates are defined by the orthonormal directions, i.e., the rolling direction (RD), the transverse direction (TD) and the normal direction (ND) of the ARB processed composites. A JEOL JSM-7001F scanning electron microscope (SEM) was used to observe the multilayered morphology on the longitudinal sections (the ND-RD plane) of the composites. Microstructures of the metals in the composites were characterized by Tecnai FEI G20 transmission electron microscope (TEM). The specimens in the RD-TD plane were carefully extracted from the plate surface at the middle thickness of the composites. The upper and bottom sides of the specimens for TEM observation were first mechanically ground and polished to a thickness of ~100 μm, and then the circular pieces with a diameter of 3 mm were punched. The specimens were mechanically thinned to 30 μm and then ion milled at −70 °C for TEM observation. X-ray diffraction (XRD) using a Rigaku SmartLab diffractometer with Cu Kα radiation (λ=0.1541 nm) was carried out on the Nb/Zr composites after the third ARB cycle to qualitatively confirm the phase composition. The composites were first ground from the both sides to reach the middle thickness of the bulk composites, and then the RD-TD planes were etched with a solution of HF (2.8 vol%), HNO_3 (4.6 vol%) and H_2O (92.6 vol%) to release the strain resulting from grinding. To reveal the texture evolution of the composites, a Rigaku Smartlab X-ray diffractometer was used to measure pole figures of each constituent metal. Measurements were also made on the RD-TD plane and at the middle thickness along the ND of the composites. The {110}, {200} and {211} pole figures of Nb and the {002}, {101}, {102} and {103} pole figures of Zr were obtained with Cu Kα radiation. The relationship between diffraction plane {*hkl*} and diffraction angle 2θ is given in Table 2. Crystallographic orientation distribution functions (ODFs) were then determined from the pole figures by the MTEX software. The notation of {*hkil*}<*uvtw*> is used for characterizing the texture type with {*hkil*} // RD-TD plane and <*uvtw*> // RD for Zr, and the notation of {*hkl*}<*uvw*> is used for Nb.

The mechanical property of the Nb/Zr multilayers was evaluated by performing uniaxial tensile tests. Dog-bone shaped tensile specimens were machined from the ARB processed composites with a wire-cut electric discharge machine and the loading direction was parallel to the RD. The surfaces and side faces of the specimens were smoothly ground to avoid the effect of the scratch on the tensile property. The specimens were then tested under uniaxial tension using a Shimadzu AG-Xplus 100kN machine at room temperature. The strain rate was 10^{-3} s^{-1}.

2 Results and Discussion

2.1 Microstructure evolution during ARB

Fig.1 shows XRD patterns of the specimens at the middle thickness of the Nb/Zr composites with different initial Zr thicknesses after the third ARB cycle. Only the diffraction peaks from Zr and Nb can be identified in the patterns. This suggests that no intermetallic phase exists in the composites even though the interdiffusion between the two metals may occur at the heterophase interfaces. Thus the fabricating route including warm rolling at 300 °C and intermittent annealing at 575 °C for the composites is reasonable in the present work. This route not only guarantees the continuous uniform plastic deformation of the composite material, but also avoids the formation of intermetallic phase at the heterophase interfaces which is harmful for the bonding of the constituent metals.

Table 1 Variation of the number of metal layers, the nominal thickness of single layer and the total strain with the increasing ARB cycles

Metal composites	Number of ARB cycles	Number of layers	Nb nominal thickness of a single layer/μm	Zr nominal thickness of a single layer/μm	Equivalent true strain
Nb-1 mm/Zr-1 mm	1	7	333	333	1.27
	2	14	111	111	2.52
	3	56	37	37	3.80
Nb-1 mm/Zr-2 mm	1	5	333	666	1.27
	2	10	111	222	2.52
	3	40	37	74	3.80

Table 2 Relationship between pole figure index {*hkl*} and diffraction angle 2θ

Nb	{*hkl*}	{110}	{200}	{211}	
	2θ/(°)	38.42	55.58	69.55	
Zr	{*hkl*}	{002}	{101}	{102}	{103}
	2θ/(°)	34.84	36.46	47.98	63.54

Fig.2 shows the lamellar morphologies of the multilayered Nb-1 mm/Zr-1 mm and Nb-1 mm/Zr-2 mm composites fabricated after different ARB cycles. The Nb layers are in grey and the Zr layers are in dark. It can be observed that the multiple layers are well bonded during the ARB processing and the heterophase interfaces between Nb and Zr are sharp

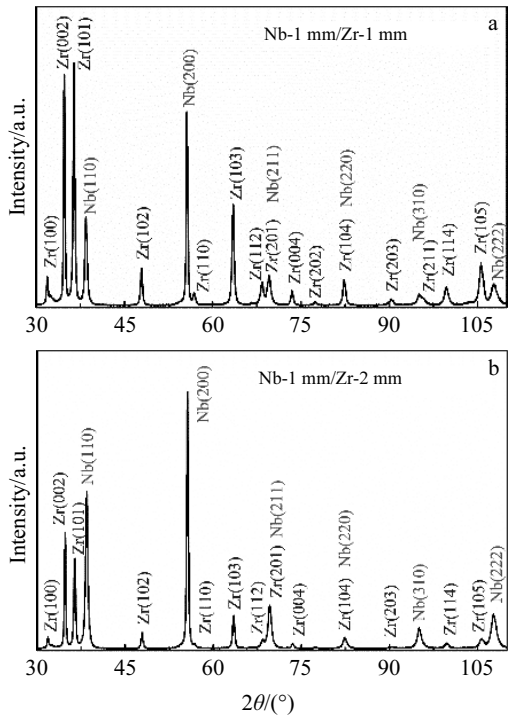

Fig.1 XRD patterns of the Nb/Zr multilayered composites processed by three ARB cycles: (a) Nb-1 mm/Zr-1 mm composite and (b) Nb-1 mm/Zr-2 mm composite

under the applied magnification for observation. With the increase of ARB cycles, the layer number increases and the thickness of the constituent layers decreases. For the multilayered metallic composites it has been well known that plastic instability preferentially occurs in the hard metal and leads to necking and fracture of the layers, because of the difference in flow stress, hardness and thickness between the constituent metals[13,16,18,33]. Meanwhile, the soft metal still remains the ability of homogeneous plastic deformation and thus is more severely elongated along the RD than the hard metal during ARB processing. Consequently, shear stress at the heterophase interfaces triggers the initiation of shear bands within the multilayered structure. The bands that are inclined to RD by approximate 30° cut through several metal layers. For the Nb-1 mm/Zr-1 mm composite (Fig.2a~2c), insignificant difference in the thickness between the constituent metals is observed and the heterophase interfaces remain straight after the first ARB cycle. Both metals are continuous along the RD, suggesting the accommodation of strain between the constituent metals at the initial stage of ARB. In addition, the thickness reduction of Zr is slightly smaller than that of Nb, due to the fact that the strength of the former metal is higher than that of the latter. After the second ARB cycle (Fig.2b), both metals remain continuous along the RD, whereas deformation in the Zr layers becomes inhomogeneous and necking occurs locally. With the increase of ARB cycles up to three, local plastic instability is caused by the different mechanical properties of the dissimilar metals. The necking region of Zr layers is seriously elongated and even fractured, leading to the significant shear banding structure within the composite. For the Nb-1 mm/Zr-2 mm composite (Fig.2d~2f), significant necking appears in Zr layers after the third ARB cycle and insignificant shear bands are observed. This indicates that the larger initial Zr layer thickness increases the accommodation of strain between the

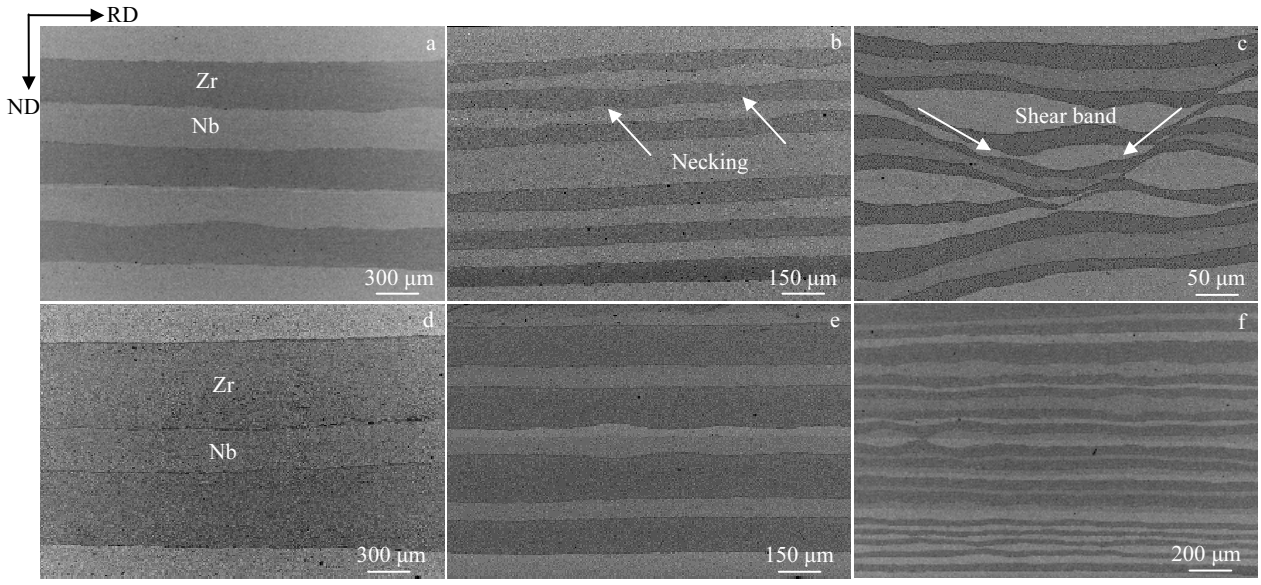

Fig.2 SEM micrographs of lamellar morphologies of the Nb-1 mm/Zr-1 mm (a~c) and Nb-1 mm/Zr-2 mm (d~f) composites processed by one (a, d), two (b, e) and three (c, f) ARB cycles

different metals and postpones the activation of shear bands.

Fig.3 shows the microstructures of the constituent metals at the middle-thickness of the Nb-1 mm/Zr-1 mm composite fabricated by three ARB cycles. The Nb layers are mainly composed of dislocation cells with different diameters, and a few dislocations can be identified in the cells (Fig.3a). In the Zr layers approximately equiaxed grains with the diameters of 200~400 nm are prominent and two features exist for the grains, i.e., some grains show high density dislocations and some other grains or subgrains show a low dislocation density induced by dynamic recovery (Fig.3b). Several large grains with the diameter larger than one micron also show a low dislocation density (Fig.3c), which is similar to the observation in Ti layers of the Cu/Ti composites produced by ARB[34]. The ARB technique is a severe plastic deformation method and can significantly refine the layers and grains within a composite. When dislocations interact and tangle with each other, the composites can be strengthened. Meanwhile, during deformation dynamic recovery reduces the dislocation density, which provides more space for the dislocation motion. Consequently, the mixed structure with the above-mentioned grain characteristics is favorable for the good combination of strength and plasticity in the composites. It should be mentioned that the melting point of Nb (T_m=2468 °C) is much higher than that of Zr (T_m=1852 °C). Therefore, the cell structure is only retained in the Nb layers with the recrystallization temperature of ~686 °C higher than the current ARB processing temperature of 575 °C, but not in the Zr layers with the recrystallization temperature of ~480 °C. The recrystallization temperature is estimated to be $0.35T_m$, where the unit of T_m is Kelvin.

2.2 Texture evolution during ARB

Fig.4 and 5 show the ODF sections with constant φ_2 for the Nb and Zr layers at the middle-thickness of the Nb-1 mm/Zr-1 mm composites, respectively. A strong texture titled about 10° away from the ideal $\{001\}<1\bar{1}0>$ orientation (rotated-Cube) and a minor {111}<112> orientation (brass-R) are found in Nb layers after the first ARB cycle. Both rotated-Cube and brass-R are the typical texture components of bcc metals under cold rolling. After the second ARB cycle, the rotated-Cube orientation is weakened and the brass-R orientation is strengthened in Nb layers, while a small amount of {001}<100> orientation (Cube) appears. With increasing ARB cycles the rotated-Cube texture continues to decrease and the Cube and brass-R textures become the dominant texture components in Nb. On the other hand, in the Zr layers the $\{10\bar{1}3\}<30\bar{3}2>$ orientation is the dominant texture after the first ARB cycle. With increasing ARB cycles, this orientation is slightly weakened and the weak $\{11\bar{2}0\}$ fiber textures located at the positions of φ_1=0~90°, ϕ=90° and φ_2=0° are evolved. This is different from the textures typically found in hcp metals under rolling, in which the basal orientation or the $\{10\bar{1}3\}<30\bar{3}2>$ orientation monotonically increases with the increased thickness reduction[35]. Fig.6 and 7 show the ODF sections for the Nb and Zr layers of the Nb-1 mm/Zr-2 mm composite processed by different ARB cycles, respectively. In comparison with the Nb/Zr composites with an initial Zr layer thickness of 1 mm, significant change in the textures in Nb layers is observed. After the second ARB cycle, the rotated-Cube orientation is still the dominant texture in Nb. After the third ARB cycle, both rotated-Cube and brass-R orientations are the main texture components, whereas the Cube orientation that dominates in the Nb-1 mm/Zr-1 mm composite is not found in Nb layers of the Nb-1 mm/Zr-2 mm composite. Comparing the composites with different initial Zr thicknesses, the texture evolution in Zr does not change significantly. Namely, the $\{10\bar{1}3\}<30\bar{3}2>$ orientation prevails and the weak $\{11\bar{2}0\}$ fiber textures also exist in Zr layers. Besides, for the composites with different initial Zr layer thicknesses, the strength of textures decreases with the increase of ARB cycles.

2.3 Mechanical property of the composites

Fig.8a and 8b show the engineering stress-strain curves of the ARB processed Nb/Zr composites under uniaxial tensile tests. For the composites with an initial Zr layer thickness of 1 mm, both yield strength and ultimate tensile strength increase with the elevated ARB numbers. After the first ARB cycle, the strength of the composite is much higher than that of pure Nb, but still lower than that of pure Zr. After the second and the third ARB cycles, the strength of the composites is higher than that of each constituent pure metal. The yield strength and tensile strength are ~475 MPa and ~640 MPa in the composite

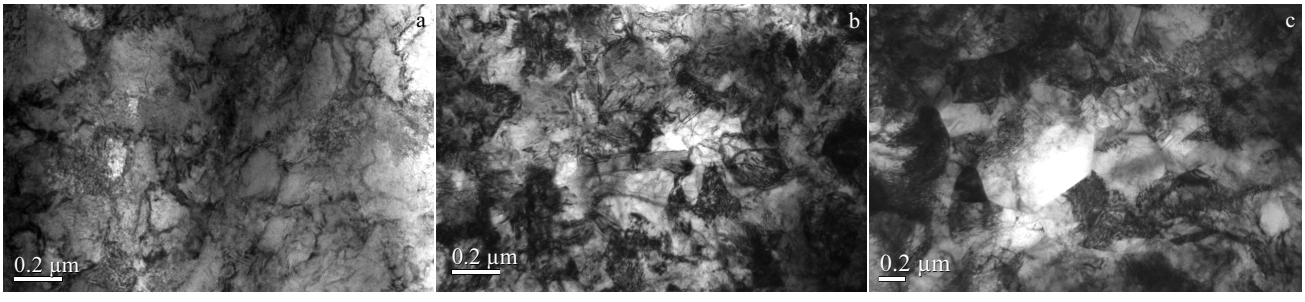

Fig.3 TEM images of the Nb-1 mm/Zr-1 mm composite processed by three ARB cycles: (a) Nb and (b, c) Zr layers

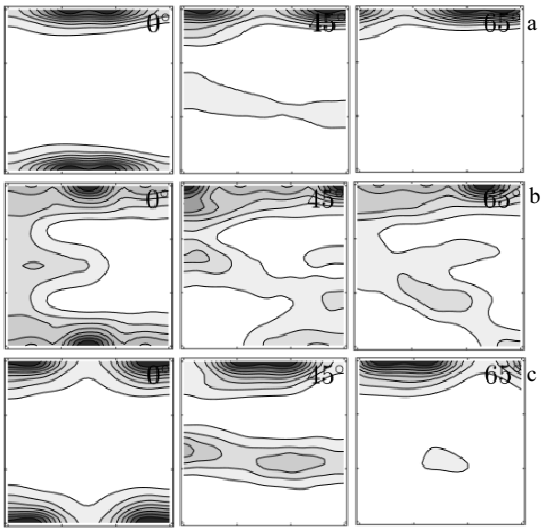

Fig.4 ODF sections with constant φ_2 (0°, 45°, 65°) in Nb at the middle thickness of the Nb-1 mm/Zr-1 mm composites processed by one (a), two (b) and three (c) ARB cycles (maximum intensity: 11.51)

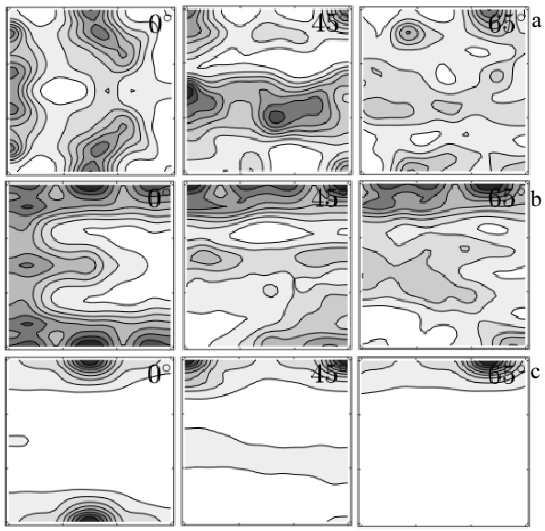

Fig.6 ODF sections with constant φ_2 (0°, 45°, 65°) in Nb at the middle thickness of the Nb-1 mm/Zr-2 mm composites processed by one (a), two (b) and three (c) ARB cycles (maximum intensity: 8.04)

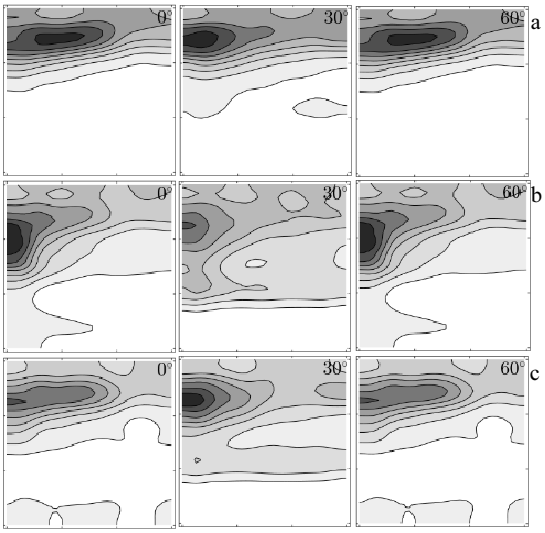

Fig.5 ODF sections with constant φ_2 (0°, 30°, 60°) in Zr at the middle thickness of the Nb-1 mm/Zr-1 mm composites processed by one (a), two (b) and three (c) ARB cycles (maximum intensity: 5.59)

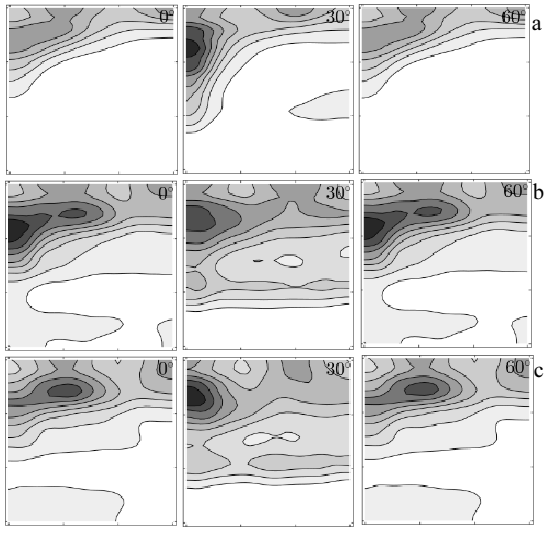

Fig.7 ODF sections with constant φ_2 (0°, 30°, 60°) in Zr at the middle thickness of the Nb-1 mm/Zr-2 mm composites processed by one (a), two (b) and three (c) ARB cycles (maximum intensity: 7.36)

processed by three ARB cycles, respectively. In addition, the composite after the first ARB cycle shows the maximum elongation of ~15.5%. When the elongation reaches ~14%, the stress decreases abruptly with the increase of strain. This is ascribed to the weak bonding of the constituent metals when the composite only undergoes one ARB cycle. Delamination within the composite results in the abrupt stress drop during tensile testing. For the composite processed by two ARB cycles, the maximum elongation is ~12%, slightly lower than that processed by one ARB cycle. After the third ARB cycle, however, the maximum elongation of the composite increases to ~14.2%. For the composites with an initial Zr layer thickness of 2 mm, the change in yield strength, ultimate tensile strength and elongation of the composite with the increasing ARB cycles show the similar tendency as that with an initial Zr layer thickness of 1 mm. After the third ARB cycle, the yield strength and ultimate tensile strength of the composite are 450 MPa and 590 MPa, respectively, and the

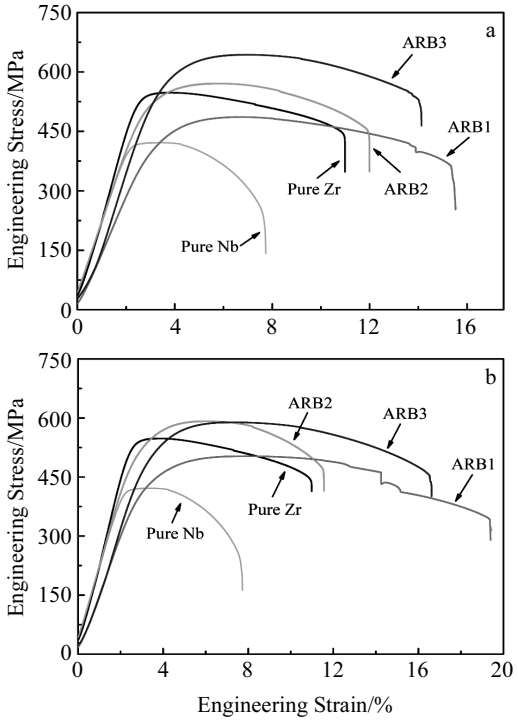

Fig.8 Engineering stress-strain curves of the Nb/Zr composites processed by different ARB cycles: (a) Nb-1 mm/Zr-1 mm composites and (b) Nb-2 mm/Zr-2 mm composites

maximum elongation attains ~16.5%. One may note that the composite with the thicker initial Zr layer shows the lower strength and the slightly higher elongation. Activation of shear banding has been postponed with increasing initial Zr layer thickness, as evidenced by the SEM observation (Fig.2). Therefore, the constituent metals in the composite with the thinner Zr layer may undergo more sever plastic deformation and thus more significant grain refinement, even though the applied thickness reductions are comparable for the two composites. In that case, the mechanical properties of the ARB processed composites are determined by the microstructures of each metal layers, and the significantly refined microstructure in the Nb-1 mm/Zr-1 mm composite leads to the higher strength but the lower plasticity.

Based on the TEM observations, dislocation density of the constituent metals in the ARB processed Nb/Zr composites is high. The dislocation entanglement increases the resistance of their motion, which results in the internal stress within the constituent metals and strengthens the bulk composites. Meanwhile, significant frictional shear strain emerges at the heterophase interfaces, due to the difference in flow stress between the constituent metals. This causes severe plastic deformation of each metal and thus significantly refines the grains. These are the reasons for the continuous increase of yield strength and ultimate tensile strength for the composites with increasing ARB cycles. It should be noted that, the warm-rolling of the composites in the present work leads to the dynamic recovery in Zr layers (shown in Fig.3). This contributes to an increase of the maximum elongation of the composite processed by three ARB cycles, instead of a significant increase of the strength. In addition, after the first ARB cycle the constituent metals could accommodate the deformation with each other, despite of their different mechanical properties. Thus the Nb/Zr composites fabricated by one ARB cycle show the largest elongations. With increasing ARB cycles, significant work hardening occurs in the composites. On the other hand, the hard metal (Zr) endures the larger stress in the composites and thus shows the less plastic deformation than the soft metal (Nb). Consequently, necking and fracture occur preferentially in the Zr layers, leading to the formation of shear bands that penetrate through several constituent layers. After more ARB cycles, the strain distribution within the composites becomes inhomogeneous due to the appearance of shear bands. This leads to the decrease in the maximum elongation of the composites. However, for the composites fabricated by three ARB cycles, it is noted that the elongation of the composites is higher than that fabricated by two cycles. This finding is different from the results reported in previous work that the maximum elongation of the multilayered metallic composites decreased rapidly to even less than 5% with increasing ARB cycles[2,9,26]. Combined with the microstructures of the constituent metals in the composites, the high dislocation density in Nb and Zr layers is responsible for the improvement in the strength of the bulk material. This is consistent with the commonly reported results for the multilayered composites produced by ARB. However, the dislocation density in some Zr grains has been reduced due to the occurrence of dynamic recovery, which is favorable for the continuous motion of dislocations under the subsequent deformation. Therefore, the tensile strength of the Nb/Zr composites increases with increasing ARB cycles whilst the ductility is not sacrificed significantly.

Meanwhile, the existence of textures may influence the micromechanical behavior of materials. For the bcc constituent within the Nb/Zr composites, different texture evolutions are observed in Nb layers as the initial Zr layer thickness changes. The strong Cube orientation in the Nb-1 mm/Zr-1 mm composite processed by three ARB cycles is in good agreement with that reported in a silicon steel under heat treatment[36], where the Cube oriented grains nucleate and grow preferentially in the shear banded area during annealing. However, under the consideration that the symmetry in a cubic lattice structure is high, the rotated-Cube and the brass-R orientations that are formed in bcc materials under conventional rolling will not bring about significant change in the tensile strength and ductility of Nb layers in comparison with the Cube orientation. For hcp materials under conventional rolling, the {0001} basal orientation or the $\{10\bar{1}3\}<30\bar{3}2>$ orientation continuously increase with the

increasing thickness reduction. Thus the activated slip systems are limited in the metals, leading to the poor ductility of the materials with those orientations[37]. In the present work, the textures in Zr layer of the ARB processed Nb/Zr composites differs from that in cold rolled pure Zr plates. Namely, the strengthening of the $\{10\bar{1}3\}<30\bar{3}2>$ orientation is insignificant and a small amount of $\{11\bar{2}0\}$ fiber textures appear in the Zr layers with increasing ARB cycles. This may be ascribed to the stress concentration at the heterophase interfaces, leading to the activation of shear bands in the multilayered structure and therefore changing the deformation mechanism of Zr. It has been generally accepted that shear bands deteriorate the ductility of metals. The formation of shear bands originates from the strong strain localization induced by complex dislocation and twin structures in a material. This process is different from the conventional activation of dislocation slip and twinning in crystalline materials and thus shows the non-crystallographic characteristic[38]. For the both Nb/Zr composites with different initial Zr layer thicknesses in this work, we show that the rotation of crystal orientation in the Zr layers is different from the texture evolution in pure hcp metals, due to the appearance of shear bands in the lamellar structure. This plays an important role in improving the uniform deformation of the multilayered metallic composites. In summary, the evolution of microstructure and texture in the ARB processed Nb/Zr composites are the decisive factors for the bulk mechanical property. The high strength and good plasticity of the composites are ascribed to the remarkable grain refinement in each constituent metal, the coexistence of grains with high dislocation density and the dynamic recovered grains in the Zr layers, together with the featured texture evolution in the Zr constituent.

3 Conclusions

1) A good interfacial bonding between the constituent metals can be achieved for the Nb/Zr composites by ARB processing. The interdiffusion between Nb and Zr occurs but no intermetallic compounds form at the heterophase interfaces. With increasing ARB cycles, shear bands that cut through multiple metal layers are more significant in the laminated structures with an initial Zr thickness of 1 mm, compared to that with an initial Zr thickness of 2 mm. Thus, in the Nb/Zr composites with the larger initial Zr thickness, necking, fracture and separation of the Zr layers are less significant than those with the smaller initial Zr thickness. Namely, the thicker Zr layer can delay the initiation of shear banding within the multilayered composites. After the third ARB cycle, dislocation cells are predominant in the Nb layers, while a mixed structure composed of grains with dense dislocations and dynamically recovered grains is found in the Zr layers.

2) Texture in the Nb layers varies with the initial Zr layer thickness of the Nb/Zr composites. For the composites with an initial Zr layer thickness of 1 mm, strong Cube orientation is formed in the Nb layers after three ARB cycles. On the contrary, for the composites with an initial Zr layer thickness of 2 mm rotated-Cube orientation is always the dominant texture in Nb at various ARB cycles, which is consistent with the rolling texture characteristic in single-phase bcc metals. Under different ARB cycles, texture evolution in the Zr layers is similar for the composites with different initial Zr layer thicknesses. After the first ARB cycle, the $\{10\bar{1}3\}<30\bar{3}2>$ orientation is dominant in the both composites. With increasing ARB cycles, this orientation is not further increased and a small amount of $\{11\bar{2}0\}$ fiber textures appear in the Zr layers. This texture evolution is different from that of pure hcp metal under rolling in which the {0001} basal orientation or the $\{10\bar{1}3\}<30\bar{3}2>$ orientation monotonically increase with the increasing thickness reduction.

3) With the increase of the ARB cycles, both yield strength and ultimate tensile strength increase for the composites with different initial Zr thicknesses. However, the maximum elongation firstly decreases and then increases with increasing roll bonding cycles. After the third ARB cycle, the maximum elongation reaches 14.2% and 16.5% for the composites with the initial Zr thickness of 1 mm and 2 mm, respectively. The significant grain refinement in the constituent metals, the coexistence of grains with high dislocation density and the dynamic recovered grains in the Zr layers, together with the texture evolution of the Zr constituent jointly contribute to the high strength and good plasticity of the ARB processed Nb/Zr composites.

References

1 Li Y P, Zhang G P. *Acta Mater*[J], 2010, 58(11): 3877
2 Wu K, Chang H, Maawad E *et al*. *Mater Sci Eng A*[J], 2010, 527(13-14): 3073
3 Bakonyi I, Péter L. *Prog Mater Sci*[J], 2010, 55(3): 107
4 Wei Q M, Liu X Y, Misra A. *Appl Phys Lett*[J], 2011, 98(11): 111 907
5 Gupta M, Amir S M, Gupta A *et al*. *Appl Phys Lett*[J], 2011, 98(10): 101 912
6 Jiang J, Godfrey A, Liu Q. *Mater Sci Tech*[J], 2005, 21(12): 1417
7 Chang H, Zheng M Y. *Rare Metal Mater Eng*[J], 2016, 45(9): 2242
8 Chen L W, Shi Q N, Chen D Q *et al*. *Mater Sci Eng A*[J], 2009, 508(1-2): 37
9 Chang H, Zheng M Y, Wu K *et al*. *Mater Sci Eng A*[J], 2010, 527(27-28): 7176
10 Zhang J Y, Li J, Liang X Q *et al*. *Sci Rep*[J], 2014, 4: 4205
11 Zhang J Y, Liu Y, Chen J *et al*. *Mater Sci Eng A*[J], 2012, 552: 392
12 Niu J J, Zhang J Y, Liu G *et al*. *Acta Mater*[J], 2012, 60(9): 3677
13 Zhang J Y, Zhang X, Liu G *et al*. *Mater Sci Eng A*[J], 2011, 528(6): 2982

14 Lee S B, Ledonne J E, Lim S C V *et al*. *Acta Mater*[J], 2012, 60(4): 1747
15 Ghalandari L, Mahdavian M M, Reihanian M *et al*. *Mater Sci Eng A*[J], 2016, 661: 179
16 Li Y P, Tan J, Zhang G P. *Scripta Mater*[J], 2008, 59(11): 1226
17 Shahabi H S, Manesh H D. *J Alloy Compd*[J], 2009, 482(1-2): 526
18 Zheng S J, Wang J, Carpenter J S *et al*. *Acta Mater*[J], 2014, 79: 282
19 Zeng L F, Gao R, Fang Q F *et al*. *Acta Mater*[J], 2016, 110: 341
20 Tirsatine K, Azzeddine H, Baudin T *et al*. *J Alloy Compd*[J], 2014, 610: 352
21 Watanbe H, Mukai T, Ishikawa K. *J Mater Sci*[J], 2004, 39: 1477
22 Zhan M Y, Li Y Y, Chen W P *et al*. *J Mater Sci*[J], 2007, 42: 9256
23 Sheikh H. *Scripta Mater*[J], 2011, 64(6): 556
24 Li X, Al-Samman T, Gottstein G. *Mater Lett*[J], 2011, 65(12): 1907
25 Ardeljan M, Savage D J, Kumar A *et al*. *Acta Mater*[J], 2016, 115: 189
26 Hosseini M, Danesh Manesh H, Eizadjou M. *J Alloy Compd*[J], 2017, 701: 127
27 Mukai T, Yamanoi M, Watanabe H *et al*. *Scripta Mater*[J], 2001, 45(1): 89
28 Xin Y C, Wang M Y, Zeng Z *et al*. *Scripta Mater*[J], 2011, 64(10): 986
29 Sandlöbes S, Zaefferer S, Schestakow I *et al*. *Acta Mater*[J], 2011, 59(2): 429
30 Callisti M, Polcar T. *Acta Mater*[J], 2017, 124: 247
31 Thompson G B, Banerjee R, Fraser H L. *Appl Phys Lett*[J], 2004, 84(7): 1082
32 Callisti M, Lozano-Perez S, Polcar T. *Mater Lett*[J], 2016, 163: 138
33 Ohsaki S, Kato S, Tsuji N *et al*. *Acta Mater*[J], 2007, 55(8): 2885
34 Jiang S, Jia N, Zhou X H *et al*. *Mater Trans*[J], 2017, 58(2): 259
35 Wang Y N, Huang J C. *Mater Chem Phys*[J], 2003, 81(1): 11
36 Sha Y H, Sun C, Zhang F *et al*. *Acta Mater*[J], 2014, 76: 106
37 Hirsch J, Al-Samman T. *Acta Mater*[J], 2013, 61(3): 818
38 Jia N, Roters F, Eisenlohr P *et al*. *Acta Mater*[J], 2013, 61(12): 4591

累积叠轧 Nb/Zr 层状复合板的微观组织与力学性能

朱明伟[1]，樊　震[2]，徐成杰[2]，贾　楠[2]

(1. 沈阳航空航天大学，辽宁 沈阳 110136)

(2. 东北大学 材料各向异性与织构教育部重点实验室，辽宁 沈阳 110819)

摘　要：采用累积叠轧法制备了初始 Zr 层厚度不同的 2 种 Nb/Zr 金属层状复合板并对其在叠轧过程中的微观结构、织构演化和力学性能进行了研究。结果显示，Nb/Zr 层状复合材料的界面结合良好，异质界面处无金属间化合物产生。随着叠轧道次增加，层状复合结构内部形成了贯穿于多个金属层的剪切带组织，初始 Zr 层厚度为 1 mm 的复合板较 Zr 层厚度为 2 mm 的复合板易于发生 Zr 层的颈缩、断裂和分离。Nb 层内主要为位错胞状结构，Zr 层内为高位错密度晶粒与动态回复晶粒的混合组织。此外，不同初始 Zr 层厚度的复合板中 Nb 层的织构演化特征不同：当初始 Zr 层厚度为 1 mm 时，Nb 表现为强立方取向；当初始 Zr 层厚度为 2 mm 时，随着叠轧道次增加，旋转立方取向始终为主导的织构组分。2 种复合板中 Zr 层的织构演化特征一致，即经 1 道次叠轧后，{0001}基面双峰织构为主要织构组分。随着叠轧道次增加，基面双峰织构略有减弱，同时出现了较弱的$\{11\bar{2}0\}$丝织构。单轴拉伸测试表明，随着叠轧道次增加 2 种不同 Zr 层厚度的复合板屈服强度和抗拉强度均逐渐增大，而塑性延伸率呈先减小后增大的趋势。经 3 道次叠轧后 2 种复合板的最大延伸率分别为 14.2%和 16.5%。叠轧过程中各金属显著的晶粒细化、Zr 层内高位错密度晶粒与动态回复晶粒共存的混合组织以及 Zr 织构的特征演化是贡献于复合板具有高强度和良好塑性的原因。

关键词：累积叠轧；Nb/Zr 层状复合材料；织构；塑性变形

作者简介：朱明伟，男，1978 年生，博士，副教授，沈阳航空航天大学材料科学与工程学院，辽宁 沈阳 110136，电话：024-89724198，E-mail: mwzhu@sau.edu.cn